JOURNAL OF AIRCRAFT
Vol. 46, No. 5, September–October 2009

Linear Damage Accumulation for Predicting Fatigue in Fiber Metal Laminates

S. U. Khan,* R. C. Alderliesten,† and R. Benedictus‡
Delft University of Technology, 2600 GB Delft, The Netherlands

DOI: 10.2514/1.42486

This paper presents the experimental and analytical research on the applicability of the linear damage accumulation approach for fatigue crack growth in fiber metal laminates under variable amplitude loading. A recently developed constant amplitude analytical prediction model for fiber metal laminates has been extended to predict fatigue crack growth under variable amplitude loading using a linear damage accumulation rule. The modified model has been compared with crack growth tests on fiber metal laminates center-cracked tension specimen. In the end, it is discussed to what extent or under which conditions the linear damage accumulation predictions are sufficiently accurate for fiber metal laminates structures.

Nomenclature

a	=	total crack length
a_D	=	delay distance
a_i	=	current crack growth increment
a_0	=	initial/total crack length of previous loading cycle
C_{cg}, n_{cg}	=	crack growth relation constants
$K_{bridging}$	=	bridging stress intensity factor
$K_{far\text{-}field}$	=	far-field stress intensity factor
K_{tip}	=	crack-tip stress intensity factor
N	=	number of loading cycles
N_D	=	number of delay cycles
N_{OL}	=	number of overload cycles
S_{max}	=	maximum stress magnitude
S_{OL}	=	overload stress magnitude
R	=	stress ratio
R_{Ktip}	=	crack-tip stress ratio
R_{OL}	=	overload stress ratio
ΔK_{eff}	=	effective stress intensity factor range

I. Introduction

FATIGUE is no doubt the main cause of failure in most load bearing components. The type of loading in nature is mainly based on variable amplitude which largely affects the severity and mechanisms of failure. In the case of metallic structures, the effect of variable amplitude (VA) loading is more pronounced due to large plastic zone sizes and crack growth retardation. On the other hand, to know about the fatigue life and crack growth in metals under VA loading, a number of prediction models have been developed [1]. These models range from simple models like linear damage accumulation (LDA) to the more complex yield zone, crack closure, and strip yield models. This variety of prediction models is the result of the required prediction accuracy. The trends of model development progress with the integration of physical phenomena like plastic zone and crack closure [2] in the formulation of the models. It has been observed that the fatigue crack growth predictions using the LDA rule are not accurate in metallic structures [3] due to the absence of consideration of plasticity and crack closure concepts. This has led to the fact that the LDA rule is unable to predict the crack growth retardation in the case of VA loading in metals.

Fiber metal laminates (FMLs), being a hybrid material of metal and composite, have metallic, composite as well as their unique properties [4]. It is assumed that LDA predictions for VA loading in FMLs are more accurate than in metals, due to the existence of fiber bridging which restrains the crack opening. As a consequence, crack closure in the wake of crack and the size of the retardation zones are supposed to be smaller than the one in monolithic metals.

II. Linear Damage Accumulation

The linear damage accumulation model is based on a cycle-by-cycle analysis independent of proceeding load cycles. It is an integration of calculated crack growth increments Δa_i using crack growth relations [5] to obtain a prediction for the full load spectrum. As a result, it is the simplest model to predict the crack growth under VA loading. The advantage of the LDA rule is computational efficiency, whereas the disadvantage is nonconsideration of nonlinear fracture mechanics concepts such as plastic zone formation in front of the crack tip, crack closure in the wake of crack, crack growth retardation, and crack growth acceleration. In general, the LDA rule can be presented mathematically as

$$a = a_0 + \sum_{i=1}^{n} f(\Delta K, r, \ldots) = a_0 + \sum_{i=1}^{N} \Delta a_i \tag{1}$$

III. Fiber Metal Laminates

After ARALL (aramid aluminum laminate) [6], GLARE (glass-reinforced) is the second member of the FML concept. Unlike ARALL, GLARE has good fatigue properties in combination with compressive loading [7]. Besides the excellent fatigue characteristics, GLARE also has good impact and damage tolerance characteristics [4]. GLARE is proved to be quite durable in case of corrosion, impact, and high temperature. The fiber/epoxy layers act as barriers against corrosion of the inner metallic sheets, whereas the metal layers protect the fiber/epoxy layers from picking up moisture. The laminate has an inherent high burn-through resistance as well as good thermal insulation properties.

FMLs are built up by alternating metal and fiber layers, as shown in Fig. 1. For standard GLARE, aluminum 2024-T3 sheets and S2-glass fibers are bonded together with FM94 epoxy adhesive to form a laminate. This stack is cured in an autoclave at 120°C and 6 bar for

Presented as Paper 2017 at the 49th AIAA/ASME/ASCE/AHS/ASC Structures, Structural Dynamics, and Materials Conference, Schaumburg, Illinois, 7–10 April 2008; received 1 December 2008; revision received 14 May 2009; accepted for publication 23 June 2009.

*Ph.D. Student, Faculty of Aerospace Engineering, Post Office Box 5058; S.U.Khan@tudelft.nl.

†Assistant Professor, Faculty of Aerospace Engineering, Post Office Box 5058; R.C.Alderliesten@tudelft.nl.

‡Professor, Faculty of Aerospace Engineering, Post Office Box 5058; R.Benedictus@tudelft.nl.

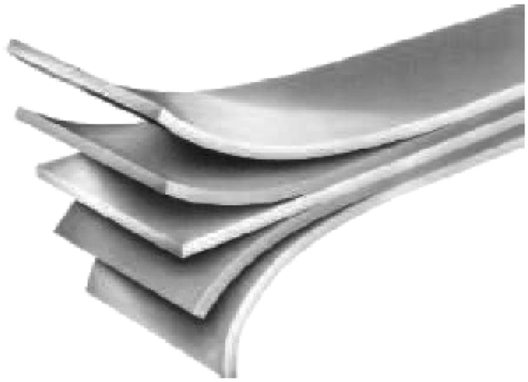

Fig. 1 GLARE.

1.5 h. The fiber orientation is defined with respect to the rolling direction of the aluminum layers and each orientation represents a prepreg layer of 0.133 mm nominal thickness. Detailed description of the ARALL and GLARE grades is shown in Table 1.

Since 1980, the FML concept has been investigated, developed, and tested, especially at Delft University of Technology. The development was sped up in 1996 after the decision of Airbus to apply GLARE on the Airbus A380 [9]. In April 2005, this newly built aircraft, with GLARE on major structural fuselage parts, performed its first maiden flight.

FML being a material made of metal and composite exhibits the properties of both metals and composites. The metallic layers show the fatigue crack growth similar to monolithic metals and the composite part shows the delamination at the metal-composite interfaces. The fibers in FMLs transfer load over the fatigue crack in the metal layers and restrain the crack opening. This phenomenon is called fiber bridging (Fig. 2). An other visible phenomenon in Fig. 2 is the occurrence of delamination at the metal–fiber interface in the wake of the crack. The cyclic shear stresses at the interface as a result of the load transfer from the metal to the fiber layers induce delamination growth. Both the fatigue crack growth in the metal layers and the delamination growth at the interfaces form a balanced and so-called coupled process.

For the development of structural FMLs, the main keys are the crack growth behavior of the metal layers and the delamination resistance of the fiber/adhesive layers. The choice of the aluminum alloy in GLARE determines to a great extent the fatigue behavior. If the metal type is determined by other (static) requirements, the fatigue behavior can only be influenced by controlling the delamination resistance of the fiber/adhesive layers [10]. Increase in delamination resistance results in better fiber bridging and thus slower crack growth in the metal layers. However, too high delamination resistance will induce too high stresses in the fiber layers, causing fiber failure. This means that control of the delamination resistance requires knowledge of the fibers and the adhesive.

IV. Selective Variable Amplitude

A selective variable amplitude load spectrum (Fig. 3) is defined as a constant amplitude spectrum with few load variations, like single overload/underload, multiple overload/underload, and their combinations in different sequences. These selective load variations are the building blocks of the (aircraft) service spectrum [11]. In the research presented here, the selective variable amplitude spectrum has been used to get the basic understanding of crack growth behavior of FMLs under aircraft spectra. These loading spectra can be categorized for understanding in the following groups.

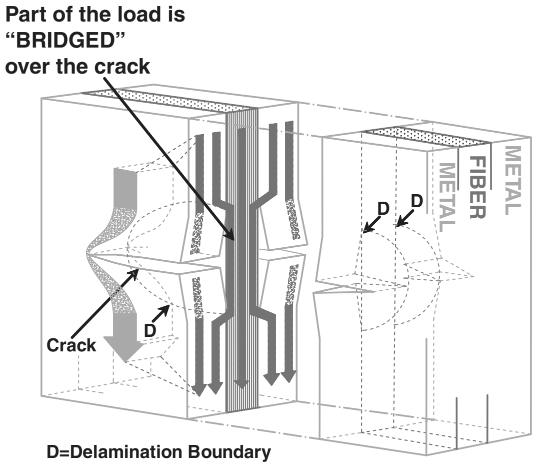

Fig. 2 Crack bridging of the fibers and delamination of the layers [8].

A. Single and Multiple Overloads

Application of a single overload (OL) in the constant amplitude (CA) baseline cycles causes a load interaction effect detailed schematically in Fig. 4. This entire mechanism is known as crack growth retardation. The magnitude and extent of the retardation is measured by the parameters defined in Fig. 4, that is, the number of delay cycles N_D, the delay distance a_D, and the OL-effected crack growth increment Δa_{OL}. Similar results and phenomena are present in case of multiple overloads. In case of single/multiple overloads, the main parameter influencing crack growth retardation is the overload ratio ($R_{\mathrm{OL}} = S_{\mathrm{OL}}/S_{\max}$). Thus, increase in R_{OL} will result in an increase in N_D, a_D, and Δa_{OL}, and a reduction in the $\mathrm{d}a/\mathrm{d}N$ level.

B. Blocks of Overloads

A block of overloads gives rise to more severe crack growth retardation during following CA baseline cycles than a single overload. Retardation occurs more rapidly than for a single overload. Similar to single overload case, the retardation effect is amplified by increasing the R_{OL}. On the other hand, an increase in the number of overload cycles N_{OL} enhances the retardation by extending the N_D period, whereas the Δa_{OL} distance remains the same as for a single overload [12,13].

C. Sequences with Underloads

Sequences having underload cycles exhibit unfavorable load interaction effects. Some investigations [14,15] revealed that highly different acceleration phenomena occur after application of an

Table 1 Commercially available fiber metal laminates [8]

	Grade	Metal type	Metal thickness, mm	Fiber layer, mm	Fiber direction, deg	Characteristics, %
ARALL	1	7075-T6	0.3	0.22	0/0	Fatigue, strength
	2	2024-T3	0.3	0.22	0/0	Fatigue, formability
	3	7475-T76	0.3	0.22	0/0	Fatigue, strength, exfoliation
	4	2024-T8	0.3	0.22	0/0	Fatigue, elevated temperature
GLARE	1	7475-T61	0.3–0.4	0.266	0/0	Fatigue, strength, yield stress
	2	2024-T3	0.2–0.5	0.266	0/0, 90/90	Fatigue, strength
	3	2024-T3	0.2–0.5	0.266	0/90	Fatigue, impact
	4	2024-T3	0.2–0.5	0.266	0/90/0, 90/0/90	Fatigue, strength in 0/90 direction
	5	2024-T3	0.2–0.5	0.266	0/90/90/0	Impact
	6	2024-T3	0.2–0.5	0.266	+45/ − 45, −45/ + 45	Shear, off-axis properties

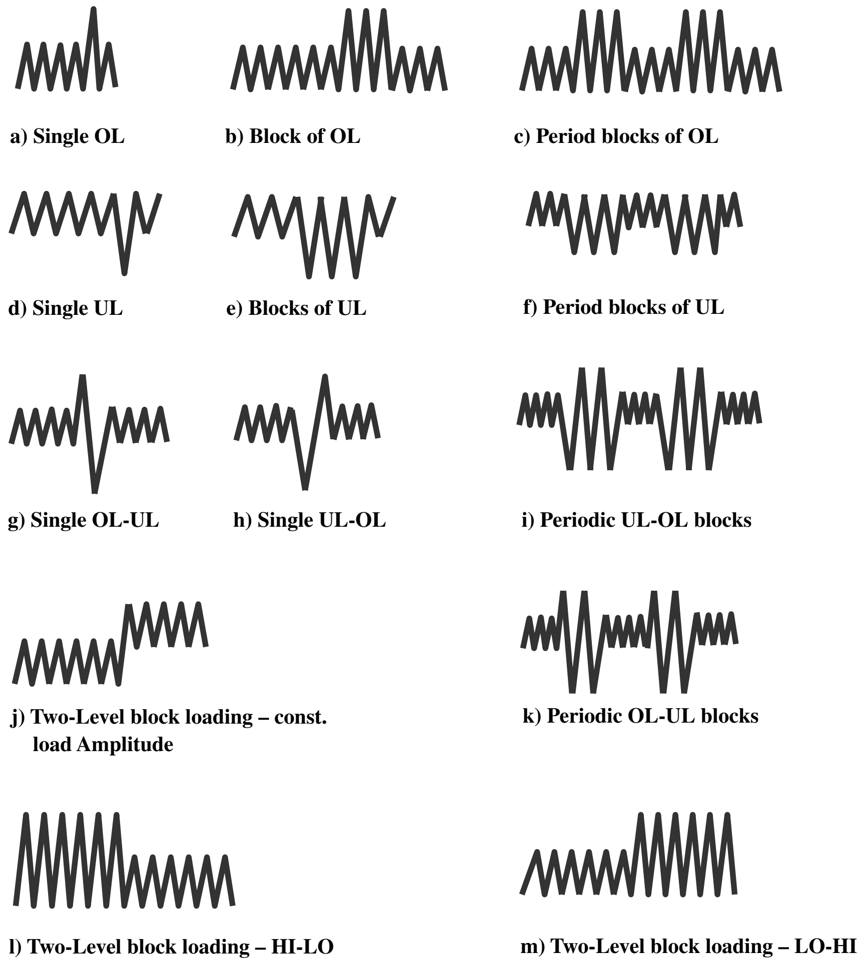

Fig. 3 Examples of selective variable amplitude load spectra [26].

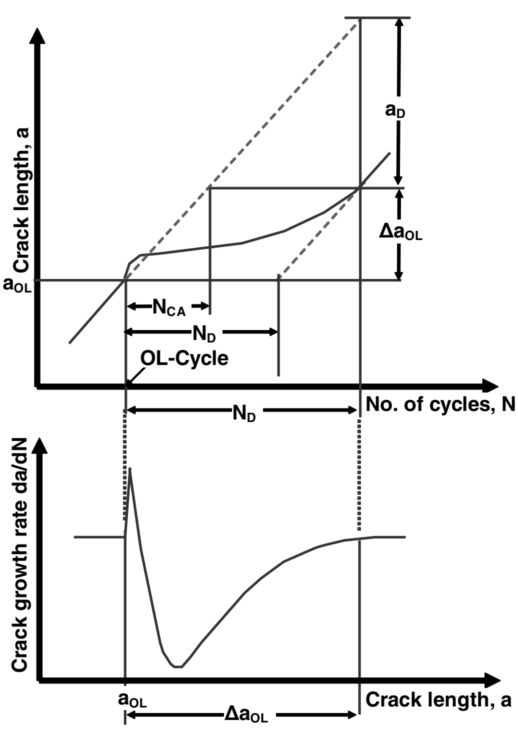

Fig. 4 Schematic of delayed retardation of crack growth following a single OL in a *K*-controlled test on metals [26].

underload in a CA baseline spectrum. A drastic increase in fatigue crack growth rate after the application of a single compressive underload has been observed in the case of uniaxial loading [16].

D. Combinations of Overloads and Underloads

In case of simple load spectra containing combinations of underload and overload cycles, the sequence has an influence on crack growth [14,17]. An underload applied just after an overload reduces the postoverload retardation, which is not the case of an overload which immediately follows an underload.

E. Two-Level Block Sequences

A high-low load sequence produces similar results as those obtained under a block of overload cycles, except that retardation in fatigue crack growth is always immediate and not preceded by the acceleration phase, whereas in the case of a low-high sequence, the start of the high-amplitude block is typically accompanied by crack growth acceleration followed by a gradual reduction until the new steady state is attained [18,19]. In some fatigue crack growth tests (Fig. 3j), only the mean load level is changed stepwise, whereas the load amplitude remains the same in each block. In such a case, a reduction of the mean load causes an immediate drop in crack growth rate below the level related to CA loading with the lower mean and crack growth retardation or even a temporary crack arrest [20].

V. Analytical Prediction Model

A model has been developed using the LDA rule [Eq. (1)] to investigate the prediction accuracy of the LDA rule for FMLs under VA loading. The CA model of Alderliesten [10,21] has been used as the basis for development of this VA prediction model using the LDA rule for FMLs. The flow diagram of the LDA prediction model is shown in Fig. 5.

The original analytical model describes the bridging stress, the delamination shape extension, the stress intensity factor, and the crack growth. It can easily be concluded from this model that the bridging stress, the crack opening contour, and the delamination shape are in balance with each other. The bridging stress is obtained by balancing the relations for the crack opening in the metal layers and the elongation and deformation of the fiber layers. The fiber layers in the FMLs transfer the load through the crack in the metal layers. Therefore, the fiber bridging stress has a direct influence on the stress intensity factor at the crack tip. However, the bridging stress is influenced by the shape of the delamination, which has a significant influence on the crack growth. Delamination growth is described using a Paris-type relation with two experimentally determined constants C_d, n_d, and the energy release rate G [22]:

$$\frac{\mathrm{d}b}{\mathrm{d}N} = C_d\left(\sqrt{G_{d,\max}} - \sqrt{G_{d,\min}}\right)^{n_d} \tag{2}$$

In the model, the effective stress intensity factor in GLARE is defined as the difference between the aluminum far-field stress intensity factor and the bridging stress intensity factor:

$$K_{\mathrm{tip}} = K_{\mathrm{far\text{-}field}} - K_{\mathrm{bridging}} \tag{3}$$

Plokker et al. [23] refined the effective stress intensity factor relation using the Schijve [24] correction (which was further improved by Rensma [25]):

$$\Delta K_{\mathrm{eff}} = (0.55 + 0.33R_{K_{\mathrm{tip}}} + 0.12R^2_{K_{\mathrm{tip}}})\Delta K_{\mathrm{tip}} \tag{4}$$

where, according to Rensma $R_{K_{\mathrm{tip}}} = K_{\mathrm{tip}_{\min}}/K_{\mathrm{tip}_{\max}}$.

Finally, the crack growth rate can be determined using the material constants C_{cg} and n_{cg} for the Paris-ΔK_{eff} region and the effective stress intensity range:

$$\frac{\mathrm{d}a}{\mathrm{d}N} = C_{\mathrm{cg}}\Delta K_{\mathrm{eff}}^{n_{\mathrm{cg}}} \tag{5}$$

To formulate this analytical approach, a program has been written using MATLAB software. The program starts with defining input variables concerning material parameters, crack geometry, and Paris constants for crack propagation and delamination growth. Other important input parameters are the spectrum file, initial delamination shape, and loading cycle counter. To make this model functional for all sorts of variable load spectra, an input file system is programmed. The spectrum file consists of stress values listed in the order of applied sequence.

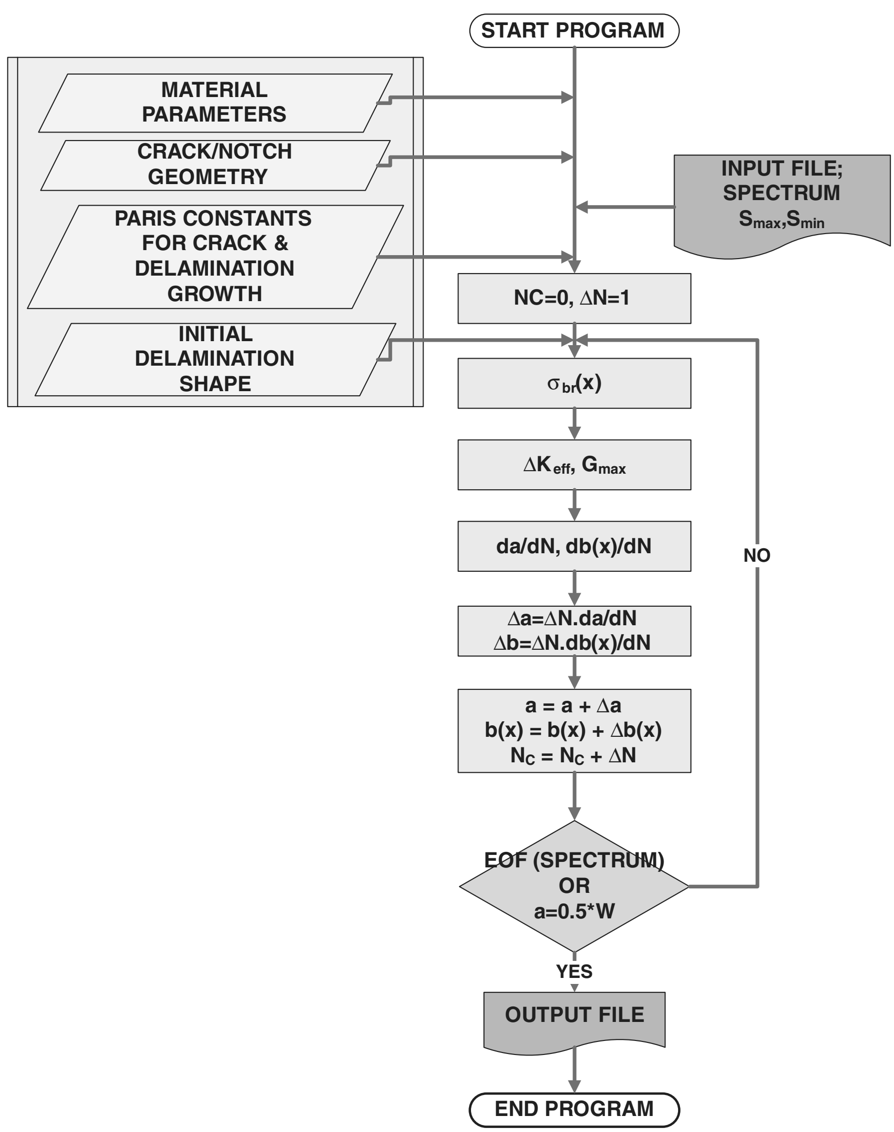

Fig. 5 Flow diagram of the LDA crack growth prediction model.

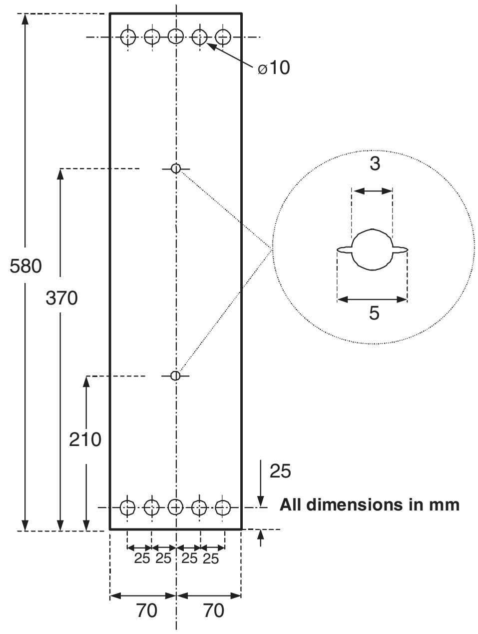

Fig. 6 Center-cracked specimen geometry.

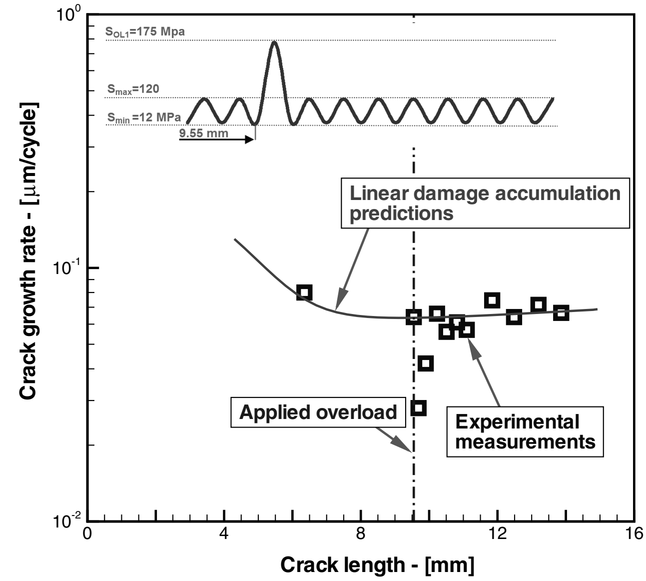

Fig. 7 Crack growth rate versus crack length for test results of CA cycles with single overload and prediction with linear damage accumulation rule.

VI. Model Validation Using Test Data

To validate the model, fatigue crack growth experiments on GLARE 3-4/3-0.3 with cross-ply fiber orientation have been performed. These fatigue crack growth tests have been performed on center-cracked tension specimens, for which the geometry is illustrated in Fig. 6. The starter notches are made by drilling a hole of 3 mm in diameter with two saw cuts, directing perpendicular to the loading direction. The total length of the starter notch ($2a_0$) is approximately 5 mm.

A. Test Matrix

The experiments were performed on specimens made of GLARE 3-4/3-0.3. Load variations are applied on a CA baseline spectrum with a maximum stress $S_{max} = 120$ MPa and a stress ratio $R = 0.1$. The single overload spectrum has an overload $S_{OL} = 175$ MPa at 100 kcycles. The multiple overload spectrum has three overloads, that is, $S_{OL1} = 175$, $S_{OL2} = 158$, and $S_{OL3} = 139$ MPa at 100, 160, and 220 kcycles, respectively. Block loading spectra have two stress levels $S_{max\,1} = 100$ MPa and $S_{max\,2} = 140$ MPa and vice versa with stress ratio $R = 0.1$. Apart from these selective VA loading spectra, representative complex flight spectra are also used for the model validation. Details of these tests are given in Table 2.

Table 2 Fatigue crack growth test matrix

Load variation	CA cycles		Load variation, MPa
	Maximum stress, MPa	Stress ratio	
Single overload	120	0.1	175
Multiple overload	120	0.1	175, 158, 139
Block loading, LO-HI	100	0.1	140
Block loading, HI-LO	140	0.1	100
Spectrum loading, I	Wide-body fuselage spectrum		
Spectrum loading, II	Megaliner front fuselage spectrum		
Spectrum loading, III	Megaliner aft fuselage spectrum		

B. Test Equipment and Procedure

The tests were conducted in lab air at room temperature on a closed-loop mechanical and computer-controlled servo-hydraulic testing system with a load capacity of 6 t. The test frequency was 10 Hz.

VII. Results and Discussion

The comparisons of LDA predictions with the tests results are shown in Figs. 7–12. Figure 7 shows the comparison for a single overload of 175 MPa in the CA baseline cycles of $S_{max} = 120$ MPa and stress ratio $R = 0.1$.

The crack growth retardation is not predicted due to the limitation of the LDA approach being a noninteraction model. The magnitude of retardation in the case of an FML is less than the monolithic metals case, making the LDA predictions slightly more reliable for FMLs. The comparison also shows that the crack growth rate gets back to the original rate as soon as the crack is out of the retardation region (which is always larger than plastic zone size).

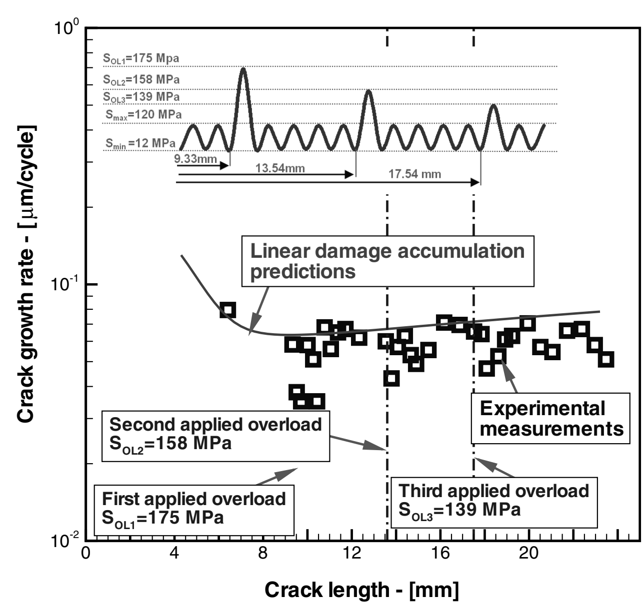

Fig. 8 Crack growth rate versus crack length for test results of CA cycles with multiple overloads and prediction with linear damage accumulation rule.

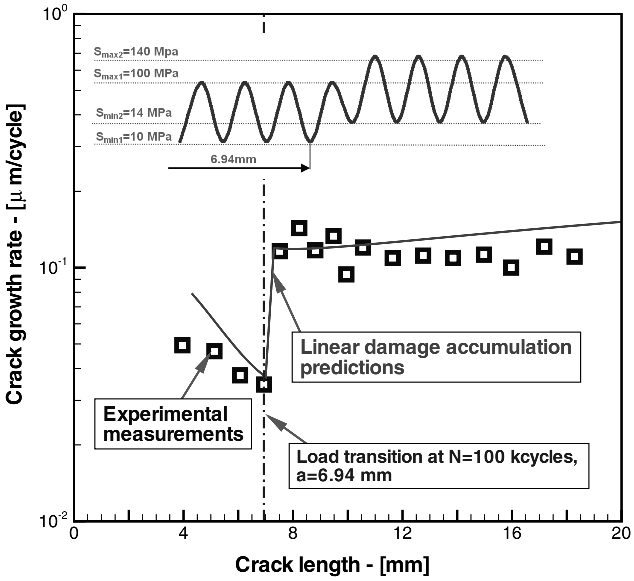

Fig. 9 Crack growth rate versus crack length for test results of low-high stress level block and prediction with linear damage accumulation rule.

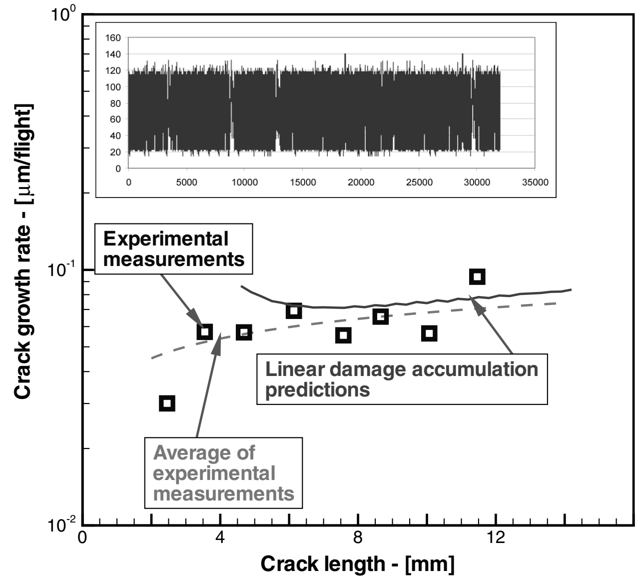

Fig. 11 Crack growth rate versus crack length for test results of spectrum I and prediction with linear damage accumulation rule.

Similar to the single overload case (Fig. 7), the crack growth rate in the multiple overload case (Fig. 8) gets back to original level depending on the magnitude of S_{OL} and R_{OL}. Figure 8 shows the comparison for the case with multiple overloads of 175, 158, and 139 MPa, respectively, in the CA baseline cycles of $S_{max} = 120$ MPa and $R = 0.1$. It is known from the literature that, in metals, the retardation region is highly influenced by the magnitude of S_{OL}, and similar behavior is seen in the case of GLARE. By reducing the S_{OL} from 175 to 158 and then to 139 MPa the crack growth retardation keeps decreasing (Fig. 8).

Figures 9 and 10 show the comparison between LDA prediction and test results for the two different sequences of block loads. The stress values are $S_{max\,1} = 100$ MPa, $R = 0.1$ and $S_{max\,2} = 140$ MPa, $R = 0.1$. Figure 9 shows the comparison for the low-high block loading case. Because the loading sequence goes from low to high values, there will not be any retardation, but due to an increase in stress level, crack growth acceleration is observed. The error in this case is less than the cases shown in Figs. 7 and 8 because the interaction effects are absent in the test.

Figure 10 shows the comparison between test results and the LDA predictions in the case of the high-low block loading sequence. The error in crack growth prediction is evident from this comparison. Because of the presence of a block of high (overload) cycles, the crack growth retardation is more than the case of a single overload. Here, it is clear that the LDA being a noninteraction model is unable to predict the crack growth and retardation.

Figures 11–13 exhibit the comparison of crack growth test results with the LDA predictions for representative complex aircraft spectra. Three different spectra are used with different S_{max} values and sequences. Spectrum I is a wide-body fuselage spectrum, whereas spectrum II is a megaliner front fuselage spectrum, and spectrum III is megaliner aft fuselage spectrum, as detailed in Table 2. The loading spectrum (spectrum II) used in Fig. 12 is a severe spectrum with a lot of variations in the stress peaks.

The observed mismatch in LDA prediction and test result for spectrum II (Fig. 12), whereas only a small error is observed for the other two spectra (Figs. 11 and 13), can be attributed to the nature of these spectra. To avoid disclosing proprietary information, only the

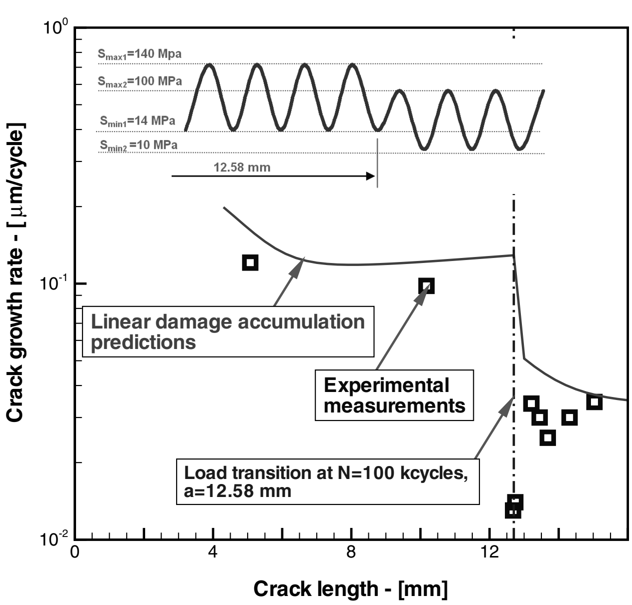

Fig. 10 Crack growth rate versus crack length for test results of high-low stress level block and prediction with linear damage accumulation rule.

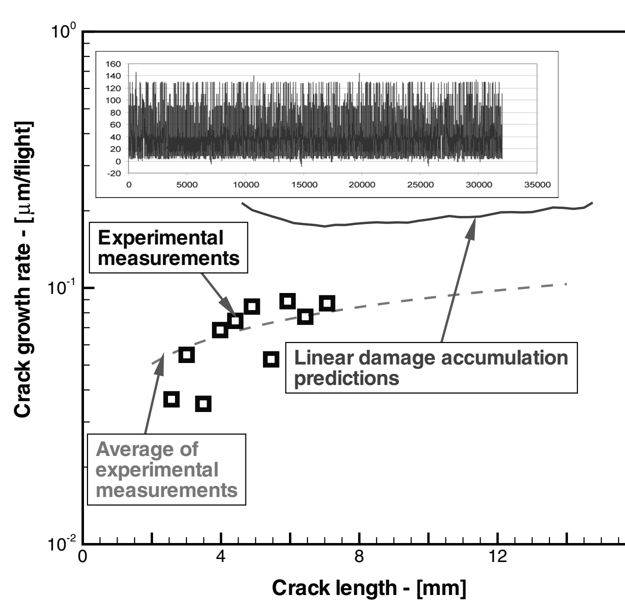

Fig. 12 Crack growth rate versus crack length for test results of spectrum II and prediction with linear damage accumulation rule.

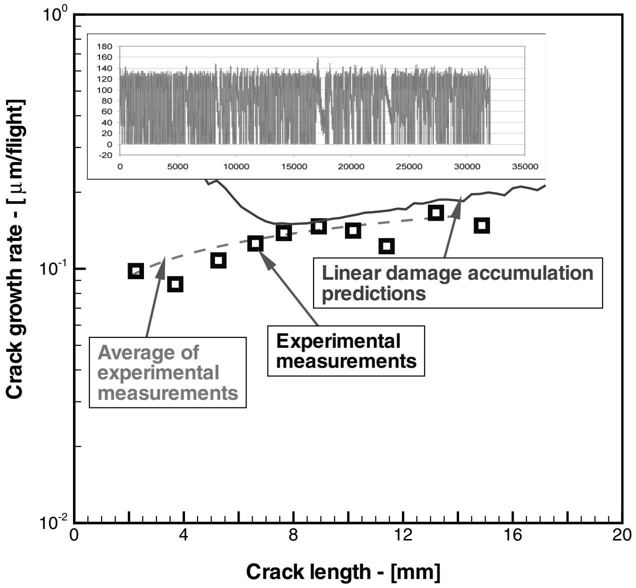

Fig. 13 Crack growth rate versus crack length for test results of spectrum III and prediction with linear damage accumulation rule.

graphical representation of the three spectra in Figs. 11–13 will be used for comparison and discussion. Comparing the spectra, one can observe that spectrums I and II have all loads randomly distributed between minimum and maximum values. Only spectrum III seems to have less amplitude cycles on the lower stress range, but that has no significant effect on crack growth, resulting in similar behavior as spectrum I. However, spectrum II has clearly large load cycles distributed throughout the spectrum with mostly stress cycles in the lower stress range. These high stresses have a retardation effect on the smaller stress cycles, which are not captured by LDA predictions.

Comparing to a single overload situation (Fig. 7), the crack in Fig. 12 seems unable to grow out of the retardation zone of previous high load in spectrum II before facing subsequent high load. This continuous retardation not captured by LDA results in the systematic mismatch.

VIII. Conclusions

A linear-damage-accumulation-based model has been introduced and evaluated with experimental results. It has been shown that the model does not predict the crack growth well when distinct load sequences occur in the applied spectrum. However, for load variations with small interaction effects and full aircraft spectra with randomly distributed load cycles, the model correlated fairly well with experimental results.

Furthermore, it has been observed from the experiments that the crack growth retardation after an overload gradually diminishes until the crack growth rate has reached its level before the application of the overload. Although different in magnitude, the phenomenon corresponds qualitatively with the behavior observed for monolithic metals. Similar to metals is the dependency of the crack growth retardation on the overload ratio R_{OL}. Small ratios result in less retardation and smaller delay zones.

Out of the three evaluated aircraft fuselage spectra, two correlated quite well with the predictions based on noninteraction. The spectrum for which the correlation was insufficient contained distinct severe peak cycles as compared to the remainder of the spectrum cycles. This might induce more distinct crack growth retardation, which is not captured by the noninteraction model. This supports the conclusion that the LDA-based prediction of crack growth in FMLs can only be accurate if the load cycles are evenly and randomly distributed throughout the applied load spectrum.

References

[1] Khan, S. U., Alderliesten, R. C., Schijve, J., and Benedictus, R., "On the Fatigue Crack Growth Prediction Under Variable Amplitude Loading," *Computational and Experimental Analysis of Damaged Materials*, 1st ed., edited by D. G. Pavlou, ISBN 978-81-7895-308-3, Research Signpost, Transworld Research Network, Kerala, India, 2007, pp. 77–105.

[2] Elber, W., "The Significance of Fatigue Crack Closure," American Society for Testing and Materials, TR STP 486, 1971.

[3] Sander, M., and Richard, H. A., "Fatigue Crack Growth Under Variable Amplitude Loading, Part II: Analytical and Numerical Investigations," *Fatigue and Fracture of Engineering Materials and Structures*, Vol. 29, No. 4, April 2006, pp. 303–319. doi:10.1111/j.1460-2695.2006.00993.x.

[4] Vlot, A., and Gunnink, J., *Fibre Metal Laminates: An Introduction*, Kluwer Academic, Dordrecht, The Netherlands, 2001.

[5] Paris, P. C., Gomez, M. P., and Anderson, W. E., "A Rational Analytic Theory of Fatigue," *The Trend in Engineering at the University of Washington*, Vol. 13, No. 1, 1961, pp. 9–14.

[6] Marissen, R., "Fatigue Crack Growth In ARALL: A Hybrid Aluminium-Aramid Composite Material," Delft Univ. of Technology, TR LR-574, 1988.

[7] Roebroeks, G. H. J. J., "Towards GLARE: The Development of a Fatigue Insensitive and Damage Tolerant Aircraft Material," Ph.D. Thesis, Delft Univ. of Technology, Delft, The Netherlands, 1991.

[8] Khan, S. U., Alderliesten, R. C., and Benedictus, R., "Post-Stretching Induced Stress Redistribution in Fiber Metal Laminates for Increased Fatigue Crack Growth Resistance," *Composite Science and Technology*, Vol. 69, Nos. 3–4, March 2009, pp. 396–405. doi:10.1016/j.compscitech.2008.11.006

[9] Vlot, A., Vogelesang, L. B., and Vries, T. F., "Toward Application of Fiber Metal Laminates in Large Aircraft," *Aircraft Engineering and Aerospace Technology*, Vol. 71, No. 6, 1999, pp. 558–570. doi:10.1108/00022669910303711

[10] Alderliesten, R. C., "Fatigue Crack Propagation and Delamination Growth in Glare," Ph.D. Thesis, Delft Univ. of Technology, Delft, The Netherlands, 2005.

[11] Schijve, J., "Prediction of Fatigue Crack Growth in 2024-T3 Alclad Sheet Specimens Under Flight-Simulation Loading," Results from a Garteur Program Memo. M-415, Delft Univ. of Technology, TR LR-574, 1981.

[12] Mills, W. J., and Hertzberg, R. W., "Load Interaction Effects on Fatigue Crack Propagation in 2024-T3 Aluminum Alloy," *Engineering Fracture Mechanics*, Vol. 8, No. 4, 1976, pp. 657–667. doi:10.1016/0013-7944(76)90039-4

[13] Chen, G. L., and Roberts, R., "Delay Effects in AISI 1035 Steel," *Engineering Fracture Mechanics*, Vol. 22, No. 2, 1985, pp. 201–212. doi:10.1016/S0013-7944(85)80022-9

[14] Ohrloff, N., Gysler, A., and Lutjering, G., "Fatigue Crack Propagation Behaviour Under Variable Amplitude Loading," *Fatigue Crack Growth Under Variable Amplitude Loading*, edited by J. Petit, D. Davidson, S. Suresh, and R. Rabbe, Elsevier Applied Science Publishers, London, 1988, pp. 24–34.

[15] Robin, C., Busch, M. L., Chergui, M., Lieurade, H. P., and Pluvinage, G., "Influence of Series of Tensile and Compressive Overloads on 316L Crack Growth," *Fatigue Crack Growth Under Variable Amplitude Loading*, edited by J. Petit, D. Davidson, S. Suresh, and R. Rabbe, Elsevier Applied Science Publishers, London, 1988, pp. 87–97.

[16] Stephens, R. I., Chen, D. K., and Hom, B. W., "Fatigue Crack Growth with Negative Stress Ratio Following Single Overloads in 2024-T3 and 7075-T6 Aluminum Alloys," American Society for Testing and Materials TR STP 595, 1976.

[17] Zhang, S., Schulte, K., Marissen, R., Trautmann, K. H., and Nowack, H., "A Systematic Fracture Surface Analysis for the Evaluation of Crack Closure Concept," *Fatigue Crack Growth Under Variable Amplitude Loading*, edited by J. Petit, D. Davidson, S. Suresh, and R. Rabbe, Elsevier Applied Science Publishers, London, 1988, pp. 48–63.

[18] Sehitoglu, H., and McDiarmid, D. L., "Effect of Load Stepdown on Fatigue Crack Arrest and Retardation," *International Journal of Fatigue*, Vol. 2, No. 2, April 1980, pp. 55–60. doi:10.1016/0142-1123(80)90032-8

[19] Ward-Close, C. M., Blom, A. F., and Ritchie, R. O., "Mechanisms Associated with Transient Fatigue Growth Under Variable Amplitude Loading: An Experimental and Numerical Study," *Engineering Fracture Mechanics*, Vol. 32, No. 4, 1989, pp. 613–638. doi:10.1016/0013-7944(89)90195-1

[20] Glinka, G., and Molski, K., "Fatigue Crack Growth Retardation Under Constant Amplitude and Variable Mean Stress," *International Journal of Fatigue*, Vol. 2, No. 3, July 1980, pp. 105–111. doi:10.1016/0142-1123(80)90011-0

[21] Alderliesten, R. C., "Analytical Prediction Model for Fatigue Crack Propagation and Delamination Growth in Glare," *International Journal of Fatigue*, Vol. 29, No. 4, April 2007, pp. 628–646. doi:10.1016/j.ijfatigue.2006.07.006

[22] Alderliesten, R. C., Schijve, J., and van der Zwaag, S., "Application of the Energy Release Rate Approach for Delamination Growth in Glare," *Engineering Fracture Mechanics*, Vol. 73, No. 6, April 2006, pp. 697–709. doi:10.1016/j.engfracmech.2005.10.006

[23] Plokker, H. M., Alderliesten, R. C., and Benedictus, R., "Crack Closure in Fiber Metal Laminates," *Fatigue and Fracture of Engineering Materials and Structures*, Vol. 30, No. 7, July 2007, pp. 608–620. doi:10.1111/j.1460-2695.2007.01140.x

[24] Schijve, J., "Some Formulas for the Crack Opening Stress Level," *Engineering Fracture Mechanics*, Vol. 14, No. 3, 1981, pp. 461–465. doi:10.1016/0013-7944(81)90034-5

[25] Rensma, E., "Investigation of Innovative Concepts for Hybrid Structures," M.S. Thesis, Delft Univ. of Technology, Delft, The Netherlands, 2007.

[26] Skorupa, M., "Load Interaction Effects During Fatigue Crack Growth Under Variable Amplitude Loading, A Literature Review, Part I: Empirical Trends," *Fatigue and Fracture of Engineering Materials and Structures*, Vol. 21, No. 8, 1998, pp. 987–1006. doi:10.1046/j.1460-2695.1998.00083.x